HHS Public Access

Author manuscript

J Nat Prod. Author manuscript; available in PMC 2016 March 27.

Published in final edited form as:

J Nat Prod. 2015 March 27; 78(3): 388–395. doi:10.1021/np500768s.

Melampodium leucanthum, a Source of Cytotoxic Sesquiterpenes with Antimitotic Activities

Andrew J. Robles[†], **Jiangnan Peng**[†,‡,*,⊥], **Rachel M. Hartley**[†,||], **Brigette Lee**[†], and **Susan L. Mooberry**[†,‡,§,*]

[†]Department of Pharmacology, The University of Texas Health Science Center at San Antonio, San Antonio, Texas 78229-3900, United States

[‡]Cancer Therapy & Research Center, The University of Texas Health Science Center at San Antonio, San Antonio, Texas 78229-3900, United States

[§]Department of Medicine, The University of Texas Health Science Center at San Antonio, San Antonio, Texas 78229-3900, United States

Abstract

A new tricyclic sesquiterpene, named meleucanthin (**1**), was isolated from an extract of the leaves and branches of *Melampodium leucanthum*, along with four known germacranolide sesquiterpene lactones, leucanthin-A (**2**), leucanthin-B (**3**), melampodin-A acetate (**4**), and 3α-hydroxyenhydrin (**5**). The chemical structure of **1** was elucidated by analysis of 1D and 2D NMR and mass spectrometric data. All compounds exhibited antiproliferative and cytotoxic efficacy against PC-3 and DU 145 prostate cancer cells, as well as HeLa cervical cancer cells, with IC_{50} values ranging from 0.18–9 μM. These compounds were effective in clonogenic assays and displayed high cellular persistence. They were also found to be capable of circumventing P-glycoprotein-mediated drug resistance. Mechanism of action studies showed that **4** caused an accumulation of cells in the G_2/M phase of the cell cycle, and **2**–**5** caused the formation of abnormal mitotic spindles. These results suggest the cytotoxic effects of these germacranolides involve inhibition of mitotic spindle function and it is likely that other mechanisms additionally contribute to cell death. These studies also demonstrate the possibility of isolating new, biologically active compounds from indigenous Texas plants.

Prostate cancer is the most common malignancy diagnosed in men in the United States and the second most common cause of cancer-related deaths.[1] In 2014, it was estimated that 233,000 new cases of prostate cancer will be diagnosed and 29,480 men will die from this

[*]**Corresponding Authors**. (S.L. Mooberry) Tel: +1 (210) 567-4788. Fax: +1 (210) 567-4300. Mooberry@uthscsa.edu. (J. Peng) Tel: +1 (910) 962-2520. PengJ@uncw.edu.

Dedicated to Dr. William Fenical of Scripps Institution of Oceanography, University of California-San Diego, for his pioneering work on bioactive natural products.

[⊥]**Present Addresses**: Department of Chemistry & Biochemistry, University of North Carolina Wilmington, Wilmington, North Carolina 28403, United States.

[||]Center for Addiction Research, The University of Texas Medical Branch at Galveston, Galveston, Texas 77555-0615, United States.

ASSOCIATED CONTENT

Supporting Information

^{1}H, COSY, HSQC and HMBS NMR spectra of compound **1**; concentration-response curves for compounds **1** – **5** in SK-OV-3 and SK-OV-3/MDR-1-M6/6 cells. This material is available free of charge via the Internet at http://pubs.acs.org

disease.[1] Only 4% of patients present with advanced disease and treatment usually includes androgen deprivation therapy. However, 10–20% of patients will develop castration-resistant prostate cancer (CRPC) within five years of their initial diagnosis.[2] Standard therapies for metastatic CRPC include combination chemotherapy with docetaxel, abiraterone, and prednisone.[3] Even with these treatment options, the median survival of patients with metastatic CRPC is a dismal 9–13 months.[4,5] Although significant strides have been made in the detection and treatment of early stage disease, there is still a critical need for more effective therapies for the treatment of late-stage and metastatic CRPC. Based on this need, we embarked on a discovery project to identify new effective treatments for prostate cancer.

Natural products have long been a major source for discovery of new drugs, especially anticancer agents. Based on recent reviews, over 60% of FDA-approved anticancer drugs are natural products, semi-synthetic compounds derived from a natural product, and/or a synthetic product designed after a natural product pharmacophore.[6,7] We sought to identify compounds cytotoxic to prostate cancer cell lines from plants that thrive in South Texas.[8–12] A total of 1086 extracts from 332 species of plants were evaluated for cytotoxic activity against PC-3 and DU 145 prostate cancer cells. A supercritical CO_2 extract from the stems and leaves of the Blackfoot daisy (*Melampodium leucanthum*, Asteraceae) was identified to have potent cytotoxic activity in both cell lines. *M. leucanthum* is a bushy, perennial plant with honey-scented flowers that is native to Texas and other parts of the southwestern U.S.

Several sesquiterpene lactones were previously isolated from this species by N. H. Fischer and colleagues.[13–19] Their studies showed that a crude syrup of *M. leucanthum* and the principal sesquiterpene lactones, melampodin A and melampodinin A, had deleterious effects on the fall armyworm, slowing larval development and causing mortality.[20] These results indicate that these sesquiterpene lactones have cytotoxic activity towards some cell types. Additionally, the Fischer laboratory previously isolated melcanthins D–G from *M. leucanthum* and identified their cytotoxic activities.[21] Previous studies have also demonstrated the cytotoxicity of a variety of sesquiterpene lactones to the human cancer cell line H.Ep. 2, as well as WI-38 human fibroblasts.[22] While the cytotoxicity of many sesquiterpene lactones has been clearly established, their cellular mechanisms of action are not well understood. Ma and colleagues previously demonstrated that several classes of sesquiterpene lactones, specifically melampolides and repandolides, inhibited nuclear factor-κB-mediated transcription in the human bone chondrosarcoma cell line SW1353 and caused G_2/M arrest.[23] However, the mechanism of G_2/M arrest was not identified and additional studies are needed to fully understand the molecular mechanisms of action of these compounds.

In this study reported is the identification of a new germacranolide isolated from *M. leucanthum*, named meleucanthin (**1**), and its antiproliferative activity has been described in several cancer cell lines. Also reported are the antiproliferative and cytotoxic activities of several other known compounds (**2**–**5**) isolated from *M. leucanthum* and the results from mechanism-of-action studies that suggest these compounds may inhibit cellular events necessary for the formation of normal mitotic spindles.

RESULTS AND DISCUSSION

Melampodium leucanthum was collected in San Antonio, Texas in June 2004. The aerial parts were quickly frozen at −20 °C, lyophilized, and then extracted with supercritical CO_2. This extract was evaluated initially for cytotoxic activity with the sulforhodamine B assay. The extract potently inhibited growth and showed cytotoxic efficacy in PC-3 and DU 145 prostate cancer cells, with IC_{50} values of 1.6 μg/mL and 1.9 μg/mL, respectively. Through bioassay-guided fractionation, the extract was separated by flash column chromatography and reversed-phase HPLC to yield a new sesquiterpene, meleucanthin (**1**) and five known germacranolides, namely, leucanthin-A (**2**), leucanthin-B (**3**), melampodin A acetate (**4**), and 3α-hydroxyenhydrin (**5**).

Compound **1** was obtained as a white gum and the molecular formula was determined as $C_{23}H_{26}O_9$ by HRESIMS (*m/z* 447.1673 $[M+H]^+$, calcd 447.1655), indicating eleven degrees of unsaturation. The ^{1}H NMR spectrum of **1** showed signals for an exomethylene at δ 6.19 (1H, d, *J* = 3.3 Hz) and 5.52 (1H, d, *J* = 3.0 Hz), two olefinic methines at δ 5.98 (1H, dd, *J* = 9.4, 5.4 Hz) and 5.39 (1H, d, *J* = 9.6 Hz), five methines at δ 5.42 (1H, d, *J* = 2.6 Hz), 4.57 (1H, t, *J* = 11.5 Hz), 3.14 (1H, dq, *J* = 11.6, 2.5 Hz), 3.05 (1H, d, *J* = 11.5 Hz), and 3.03 (1H, d, *J* = 6.6 Hz), and five methyl groups at δ 3.63 (3H, s), 2.08 (3H, s), 2.04 (3H, s), 1.55 (3H, s), 1.25 (3H, d, *J* = 5.4 Hz). The signal at δ 5.71 (2H, m) was determined to be one olefinic methine and one oxygenated methine from the HSQC spectrum. Since only a small quantity of **1** was isolated, the ^{13}C NMR spectrum was not obtained, and the ^{13}C NMR data were extracted from the HSQC and HMBC spectra. In addition to the aforementioned groups, quaternary carbons, including four carbonyl carbons, two olefinic carbons and two aliphatic carbons, were indicated by the ^{13}C NMR data. These data together with 2D NMR data (Figure 1) were consistent with a 6,12-eudesmanolide type sesquiterpene lactone skeleton. The methyl carboxylate group at C-14 was determined from the signal at the δ_C 169.8 (C-14) and its HMBC correlations with H-1, H-5, and H-9. An acetoxy group (δ_H 2.09 (3H, s); δ_C 168.2 and 20.4) was assigned to C-9 by the HMBC correlation of H-9 with the carbonyl carbon. A 2,3-epoxy-2-methylbutyryloxy group was deduced from the ^{1}H and ^{13}C NMR data and was assigned at C-8 based on the HMBC correlation between H-8 and C-1′. The relative configuration of this group was determined as 2′*S**,3′*S** by comparing its ^{1}H and ^{13}C NMR data with literature values.[18,19] The large coupling constants (ca. 12 Hz) between H-5/H-6, H-6/H-7 indicated the axial-axial relationship between these protons, while the small coupling constants (2.6 Hz) between H-7/H-8 and H-8/H-9 suggested the axial-equatorial relationship of these protons. Thus, the structure of **1** was determined as depicted, and the trivial name meleucanthin was assigned. The absolute configuration was not determined because of the limited quantity of material. The structures of compounds **2**–**5** were determined by spectroscopic methods (2D NMR and MS) and comparison with literature data.[13–19,21]

The antiproliferative and cytotoxic activities of **1**–**5** were evaluated in the PC-3 and DU 145 prostate cancer cell lines, and the HeLa cervical cancer cell line using the sulforhodamine B (SRB) assay. Compound **1** proved to be the most potent cytotoxin of this series, with IC_{50} values of 0.67 μM and 0.18 μM in PC-3 and DU 145 cells, respectively (Table 1). The 3.7-fold difference in IC_{50} values for 1 in these two cell lines contrasted to the effects of **2**–**5**,

which had similar potencies in each cell line evaluated (Table 1). Compounds **2** –**5** had similar potencies and shapes of the concentration-response curves in PC-3, DU 145, and HeLa cells (Figure 2). DU 145 cells were more sensitive to most of the compounds than PC-3 cells, except for **3**, which was slightly more potent in PC-3 cells (Table 1). The concentration-response curves for the compounds in each cell line also indicated that all of the compounds were cytotoxic, and not simply antiproliferative (Figure 2). This was not observed with all cytotoxins, as demonstrated with the control compound paclitaxel. While paclitaxel was highly potent and efficacious in DU 145 and HeLa cells, it was only cytostatic in PC-3 cells at the concentrations tested as is indicated by the plateau of the curve at 60% inhibition relative to control. Cytotoxicity was measured by a decrease in cell density from that measured at the time of drug addition. Interestingly, while **2**–**5** showed very similar potency in both prostate cancer cell lines, the potency of **1** was 3.7-fold greater in DU 145 cells than PC-3 cells, suggesting the mechanisms of action for **2**–**5** are different than that of **1**. However, it is worth noting that while the concentration-response curves for **2** and **4** were nearly identical in these three cell lines, the curves for **3** and **5** showed small differences among the cell lines. This suggests that there may be slight differences in the mechanisms of action of these two groups of compounds. It is also interesting that **4**, the most potent of the four known compounds obtained, does not have an epoxide at C-4/C-5 (carbon numbers refer to those established by Fischer et al.) while **2**–**4** do. This indicates that this functional group is not necessary for mediation of the cytotoxic activity of these compounds. Examining the structural and potency differences between **2** and **5** also indicates that a hydroxy group at C-3 may be detrimental to the potency of this class of compounds since **5** is much less potent than **2**–**4**. We next asked the question if these compounds are selectively cytotoxic to cancer cells by evaluating **2**–**4** in the A-10 rat smooth muscle cell line. Compounds **2**–**4** had similar potencies in this cell line compared to the cancer cell lines, indicating that the mechanism of action of these compounds is not specific to cancer cells (Table 1 and Figure S2, Supporting Information). The limited yield of **1** precluded additional biological experiments.

The cellular persistence of **2**–**5** was evaluated in DU 145 cells by determining their ability to inhibit colony formation after drug washout. This experimental paradigm evaluates the long-term effects of a compound after a short exposure. Several studies have suggested that cellular persistence can help predict efficacy in vivo.[24,25] Compounds that have a high level of cellular persistence or initiate their cellular effects very quickly may be less susceptible to pharmacokinetic liabilities. The cellular persistence of **2**–**5** was evaluated using a clonogenic assay in which cells were exposed to compound for 4 h. Compounds **2**–**5** all caused a dose-dependent and statistically significant decrease in colony formation relative to vehicle-treated controls (Figure 3A and B). Representative pictures of colonies following treatment with vehicle or 5, 10 or 20 μM of **5** are shown in Figure 3A. The bar graph in Figure 3B shows the effects of compounds **2**–**5** on colony formation as an average of multiple experiments. These results demonstrate that the compounds have a high degree of cellular persistence and can induce cytotoxicity after short treatment times, leading to inhibition of colony formation after nine days. Additionally, they show that compounds **2** and **4** are the most potent at inhibiting colony formation, which is consistent with the data obtained in the SRB experiments.

The ability of **2**–**5** to initiate apoptosis after 24 h was evaluated by caspase-mediated PARP cleavage. HeLa and DU 145 cells were treated with vehicle, the positive control BI2536 (100 nM) or **2**–**5** (10 μM). PARP cleavage was evaluated by immunoblotting. Robust PARP cleavage was observed in the positive control in HeLa cells (Figure 4) and with each of the compounds. The highest levels of PARP cleavage were seen with compounds **4** and **5** in HeLa and with **2** and **3** in DU 145, consistent with the results for the positive control in that different cells respond to apoptotic stimuli differently.

A common problem with the treatment of cancer is the development of multidrug resistance and drugs that can overcome drug resistance mechanisms, including expression of P-glycoprotein (Pgp) efflux pump, which removes many foreign molecules from cells and can lead to low, ineffective cellular concentrations of drug molecules. The ability of **2**–**5** to circumvent Pgp-mediated drug resistance was studied using an isogenic ovarian cancer cell line pair, the parental SK-OV-3 line and the Pgp-expressing clone SK-OV-3/MDR-1-M6/6 (M6/6). While the IC_{50} of the known Pgp substrate paclitaxel was significantly higher in the M6/6 cells than SK-OV-3 cells, with a relative resistance (Rr) factor of 162.9, the sensitivity of the M6/6 cells to **2**–**5** were only slightly lower than in the parental cells, with Rr values ranging from 2.1 to 2.6 (Table 2 and Figure S1, Supporting Information). These results show that **2**–**5** are effective in Pgp-expressing cells and appear to be poor substrates for Pgp.

Many anticancer agents induce changes in cell cycle distribution related to their mechanisms of action. To investigate the cellular mechanisms of action of **2** and **4**, their effects on cell cycle distribution were evaluated in PC-3 cells by flow cytometry. After an 18 h treatment, concentrations as high as 5 μM of **2** caused no significant changes in the cell cycle distribution compared to control (Figure 5). However, 3 μM of **4** caused an accumulation of cells in the G_2/M (Figure 5), suggesting the possibility of antimitotic effects. To determine if these compounds directly interact with tubulin, a known antimitotic target, the effects of **2**–**5** on purified tubulin polymerization was evaluated. All four compounds caused a slight inhibition of tubulin polymerization at concentrations significantly higher than their IC_{50} values for growth inhibition and cell death (Figure 6). This is not unexpected because the concentrations of known tubulin binding agents that are needed to inhibit purified tubulin polymerization greatly exceed the IC_{50} values for cytotoxicity in cells. This was also the case with the positive control colchicine. These results suggest that **2**–**5** can modestly inhibit tubulin polymerization, but that they might have additional actions. We next evaluated the effects of **2**–**5** on cellular microtubules. The effects of **2**–**5** on mitotic spindles, microtubules and overall cellular morphology were evaluated by indirect immunofluorescence microscopy. Vehicle-treated HeLa cells displayed normal interphase microtubules morphologies, and the majority of mitotic cells had normal, bipolar spindles (Figure 7A). In contrast, treatment with **2**–**5** resulted in a slight accumulation of mitotic cells, with most cells displaying either monopolar mitotic spindles or aberrant bipolar mitotic spindles (Figure 7C–F). This is not the typical phenotype of microtubule depolymerizing agents, but was similar to that seen with treatment of the polo-like kinase 1 (PLK-1) inhibitor BI 2536, which leads to accumulation of a large number of cells with monopolar mitotic spindles surrounded by a circle of chromosomes (Figure 7B). However, **2**–**5** caused noticeably less accumulation of mitotic cells with this phenotype with a range of concentrations. Similar

results were also observed with PC-3 cells after treatment with **2**–**5**. To investigate whether these compounds inhibit PLK1, HeLa and DU 145 cells were treated with vehicle, 100 nM BI 2536 or 10 of μM **2**–**5**, lysed, and evaluated by immunoblotting for PLK1 and phospo-Thr210-PLK1. As previously demonstrated,[26] BI2536 caused an accumulation of both PLK1 and phospo-Thr210-PLK1(data not shown). In contrast, no increase in PLK1 or phospo-Thr210-PLK1 was observed after treatment with **2**–**5**, indicating that PLK1 inhibition is not a primary mechanism of action of these compounds (data not shown). Together these data suggest that while these compounds are capable of inhibiting normal mitotic spindle formation at cytotoxic concentrations, inhibition of PLK1 does not appear to be their mechanism of action. Multiple cellular mechanisms may be responsible for these aberrant mitotic spindles and for the cytotoxic effects of these compounds.

In summary, described herein are the isolation of a new, tricyclic sesquiterpene and the evaluation of its antiproliferative and cytotoxic activities. Additionally, four previously identified germacranolides were isolated and their cellular mechanisms of action investigated in cancer cell lines. These studies demonstrate for the first time that **2**–**5** inhibit normal mitotic spindle formation and that compound **4** additionally inhibits mitotic progression. These compounds can act directly with tubulin, yet cause only minimal effects on inhibition of tubulin polymerization, suggesting the possibility of additional targets. Further studies will be needed to more completely characterize the cellular effects of these compounds and determine whether multiple targets are involved.

EXPERIMENTAL SECTION

General Experimental Procedures

The UV spectrum was obtained online with a Waters 996 PDA detector. NMR spectra were recorded on Bruker Avance 600 MHz or 500 MHz instruments. All NMR data were measured and reported in ppm using TMS as an internal standard. The HRESIMS was measured using an Agilent Technologies 6224 TOF LC/MS mass system. TLC was performed on aluminum sheets (silica gel 60 F254, Merck KGaA, Germany). Preparative HPLC was performed on a Waters Breeze HPLC system using a Phenomenex Luna C_{18} column (250 × 22.5 mm, 5 μm). A gradient elution was utilized starting from 40% MeOH-H_2O to 100% MeOH in 40 min with a flow rate of 9 mL/min. LC/MS was conducted on a Waters Alliance 2695 HPLC equipped with Micromass Quattro triple quadrupole mass spectrometer using the ESI mode.

Plant Material

The aerial parts of *Melampodium leucanthum* were collected in San Antonio, Texas in June 2004. The plant material was collected, quickly frozen at −20 °C, and then lyophilized. Voucher specimens (SLM009) were deposited in our herbarium and authenticated by Mr. Paul Cox, former superintendent of the San Antonio Botanical Gardens.

Extraction and Isolation

Lyophilized and pulverized aerial plant parts (73 g) were extracted with supercritical CO_2 alone followed by extraction with supercritical CO_2 and MeOH. The extract generated with

CO_2 only (500 bar at 50 °C) was effective against PC-3 and DU 145 prostate cancer cells while the CO_2 and MeOH extract showed no effects at 25 μg/mL. The CO_2 extract (1.4 g) was subjected to flash chromatography on silica gel columns (Biotage SNAP KP-Sil 50g) and eluted with a methylene chloride and acetone (0 ~ 15%) gradient. Fractions were combined and screened for cytotoxicity against PC-3 prostate cancer cells using the SRB assay. Only the active fractions were further purified. Fraction 3 was repeatedly chromatographed on preparative HPLC eluted with a gradient of 40% MeOH-H_2O to 100% MeOH to yield compounds **1** (1.2 mg) and **2** (5.5 mg). Fraction 5 was separated on preparative HPLC using the same conditions to yield compounds **3** (22.1 mg) and **4** (8.2 mg). Similarly, compound **5** (4.8 mg) was obtained from fraction 8 after purification by HPLC.

Compound **1**: white gum, UV λ_{max} 221 nm; ^{1}H NMR (500 MHz, $CDCl_3$) δ 6.19 (1H, d, *J* = 3.3 Hz, H-13a), 5.98 (1H, dd, *J* = 9.4, 5.4 Hz, H-2), 5.71 (2H, m, H-3,8), 5.52 (1H, d, *J* = 3.0 Hz, H13b), 5.42 (1H, d, *J* = 2.6 Hz, H-9), 5.39 (1H, d, *J* = 9.6 Hz, H-1), 4.57 (1H, t, *J* = 11.5 Hz, H-6), 3.63 (3H, s, OCH_3), 3.14 (1H, dq, *J* = 11.6, 2.5 Hz, H-7), 3.05 (1H, d, *J* = 11.5 Hz, H-5), 3.03 (1H, d, *J* = 6.6 Hz, H-3′), 2.08 (3H, s, Ac), 2.04 (3H, s, H-15), 1.55 (3H, s, H-5′), 1.25 (3H, d, *J* = 5.4 Hz, 4′); ^{13}C NMR (125 MHz, $CDCl_3$) δ 169.8 (C-14), 169.0 (C-11), 168.3 (Ac), 168.2 (C-1′), 138.6 (C-4), 132.9 (C-12), 125.6 (C-2), 121.6 (C-1), 120.6 (C-13), 117.5 (C-3), 76.2 (C-6), 72.7 (C-9), 67.3 (C-8), 60.1 (C-3′), 59.1 (C-2′), 52.8 (C-10), 52.3 (OCH_3), 45.8 (C-7), 43.0 (C-5), 23.5 (C-15), 20.4 (Ac), 18.9 (C-5′), 13.5 (C-4′); HRMS *m/z* 447.1673 [M+H]+ (calcd 447.1655); ESI-MS *m/z* 447.1 [M+H]+, 469.1 [M+Na]+.

Cell Culture

DU 145 and PC-3 prostate cancer cells and HeLa cervical cancer cells were purchased from the American Type Culture Collection (Manassas, VA, USA). DU 145 cells were cultured in Improved Minimum Essential Medium (IMEM) (Gibco) with 10% FBS and 25 μg/mL gentamicin, PC-3 cells were cultured in RPMI 1640 medium (Sigma-Aldrich) with 10 % FBS and 50 μg/mL gentamicin, and HeLa cells were cultured in Basal Medium Eagle (BME) with Earle's salts (Sigma-Aldrich) with 10% FBS and 50 μg/mL gentamicin. The SK-OV-3/MDR-1-6/6 cell is a single-cell clone isolated from the SK-OV-3/MDR-1 cell line, and was provided by S. Kane (Division of Molecular Medicine, Beckman Research Institute of the City of Hope, Duarte, CA, and cultured as previously described.[24–25]

In vitro Antiproliferative/Cytotoxicity Assays

The in vitro antiproliferative and cytotoxic effects of **1**–**5** in each cell line were evaluated using the sulforhodamine B (SRB) assay as previously described.[27,28] IC_{50} values, defined as the concentration resulting in 50% inhibition of cell proliferation compared to vehicle-treated control, were interpolated from 4-parameter nonlinear regressions of the concentration-response curves using Graphpad Prism 6. All data represent the mean ± SE.

In Vitro Clonogenic Assays

DU 145 cells (300) were allowed to adhere in 60 mm^3 tissue culture dishes and subsequently treated with vehicle (final concentration of 0.5% DMSO) or compounds **2**–**4**. After 4 h of treatment, cells were washed with Dulbecco's phosphate-buffered saline (DPBS) and fresh

growth medium was added. After 14 days, cells were fixed and stained with 0.5% crystal violet in 10% methanol. Colonies were counted using GeneSnap software (PerkinElmer). Data were analyzed by one-way ANOVA with Dunnett's post-hoc test using GraphPad Prism 6.

Immunoblotting/Cell Lysates

DU 145 cells were treated with vehicle, or compounds **2–4** for various time periods, as indicated, and then the cells were harvested and lysed with cell extraction buffer (Invitrogen) containing protease inhibitors. The total protein concentrations were measured and equal amounts of protein were separated by SDS-PAGE and transferred to a PVDF membrane. Membranes were probed for actin (1:5000; Sigma-Aldrich) or cleaved PARP (1:1000; Cell Signaling). Signals were visualized with Amersham ECL Plus (GE Health Care) in a Geliance (PerkinElmer) imaging system.

Tubulin Polymerization Assay

Purified porcine tubulin (Cytoskeleton, Inc.) polymerization was monitored turbidimetrically by measuring the absorbance at 340 nm using a SpectraMax Plus 384 spectrophotometer (Molecular Devices). Tubulin (2 mg/mL) was dissolved in GPEM buffer (Cytoskeleton, Inc.) containing 80 mM PIPES (pH 6.8, 1 mM $MgCl_2$, 1 mM EGTA, 10% glycerol) and 1 mM GTP and incubated with vehicle (1% DMSO v/v), colchicine, or **2**–**5** for 1 h at 37 °C.

Flow Cytometry

The effects of each compound on cell cycle distribution were evaluated using flow cytometry. PC-3 cells were treated with vehicle (DMSO) or compounds **1**–**4** for 18 h. Cells were then harvested, stained with Krishan's reagent, and their DNA content was analyzed using a FACSCalibur flow cytometer (BD Biosciences).

Immunofluorescence Microscopy

PC-3 and HeLa cells were plated onto glass coverslips and allowed to adhere overnight before compound addition. After treatment with the compounds for 18 h, cells were fixed with methanol (4 °C) for 5 min and subsequently incubated with a blocking solution of 10% bovine calf serum in DPBS for 20 min at room temperature. Cells were then incubated with a monoclonal β-tubulin antibody (1:400; Sigma T4026) for 2 h at 37 °C. After incubation, cells were washed three times with 1% bovine serum albumin (BSA) in DPBS and then incubated with a FITC-conjugated sheep anti-mouse IgG (1:200; Sigma F3008) for 1 h at 37°C. Coverslips were then washed three times with BSA in PBS and stained with 0.1 μg/mL DAPI (Sigma D9564) in DPBS for 10 min at room temperature. Coverslips were mounted on slides and visualized with an Eclipse 80i fluorescence microscope with a Plan Apo VC 60× H objective (Nikon). Images were captured with a CoolSNAP HQ2 camera (Photometrics) using NIS Elements software (Nikon).

Supplementary Material

Refer to Web version on PubMed Central for supplementary material.

Acknowledgments

The authors thank Paul Cox for his help identifying the *M. leucanthum* samples used in this study and Gary A. Fest for his technical assistance.

Funding Sources

This study was supported by grants to S.L.M. from the CDMRP Prostate Cancer Program (W81XWH-08-1-0395), the UTHSCSA President's Council Excellence Award, and the Greehey Distinguished Chair in Targeted Molecular Therapeutics. Support of the Flow Cytometry, Macromolecular Structure and Mass Spectrometry Shared Resources of the CTRC Cancer Center Support Grant (P30 CA054174) are gratefully acknowledged. Andrew Robles was supported by the IMSD program of the NIGMS (1R25GM095480-01). Rachel Hartley was supported by the COSTAR program NIDCR (DE14318), and T32 training grant (CA148724).

REFERENCES

1. Siegel R, Ma J, Zou Z, Jemal A. CA Cancer J. Clin. 2014; 64:9–29. [PubMed: 24399786]
2. Kirby M, Hirst C, Crawford ED. Int. J. Clin. Pract. 2011; 65:1180–1192. [PubMed: 21995694]
3. Cookson MS, Roth BJ, Dahm P, Engstrom C, Freedland SJ, Hussain M, Lin DW, Lowrance WT, Murad MH, Oh WK, Penson DF, Kibel AS. J. Urol. 2013; 190:429–438. [PubMed: 23665272]
4. Hwang SS, Chang VT, Alejandro Y, Mulaparthi S, Cogswell J, Srinivas S, Kasimis B. Cancer. Invest. 2004; 22:849–857. [PubMed: 15641482]
5. Soerdjbalie-Maikoe V, Pelger RC, Lycklama a Nijeholt GA, Arndt JW, Zwinderman AH, Bril H, Papapoulos SE, Hamdy NA. Eur. J. Nucl. Med. Mol. Imaging. 2004; 31:958–963. [PubMed: 14985870]
6. Newman DJ, Cragg GM. J. Nat. Prod. 2012; 75:311–335. [PubMed: 22316239]
7. Pan L, Chai HB, Kinghorn AD. Front. Biosci. (Schol Ed). 2012; 4:142–156. [PubMed: 22202049]
8. Hartley RM, Peng J, Fest GA, Dakshanamurthy S, Frantz DE, Brown ML, Mooberry SL. Mol. Pharmacol. 2012; 81:431–439. [PubMed: 22169850]
9. Li J, Risinger AL, Peng J, Chen Z, Hu L, Mooberry SL. J. Am. Chem. Soc. 2011; 133:19064–19067. [PubMed: 22040100]
10. Peng J, Hartley RM, Fest GA, Mooberry SL. J. Nat. Prod. 2012; 75(3):494–496. [PubMed: 22260294]
11. Peng J, Jackson EM, Babinski DJ, Risinger AL, Helms G, Frantz DE, Mooberry SL. J. Nat. Prod. 2010; 73:1590–1592. [PubMed: 20715765]
12. Peng J, Risinger AL, Fest GA, Jackson EM, Helms G, Polin LA, Mooberry SL. 2011; 54:6117–6124.
13. Fischer NH, Seaman FC, Wiley RA, Haegele KD. J. Org. Chem. 1978; 43:4984–4987.
14. Fischer NH, Wiley RA Jr, Huei-Nan L, Karimian K, Politz SM. Phytochemistry. 1975; 14:2241–2245.
15. Fischer NH, Wiley R, Wander JD. Journal of the Chemical Society Chemical Communications. 1972:137–139.
16. Fischer NH, Wiley RA, Perry DL, Haegele KD. J. Org. Chem. 1976; 41:3956–3959.
17. Olivier EJ, Perry DL, Fischer NH. J. Org. Chem. 1980; 45:4028–4034.
18. Quijano L, Fronczek FR, Fischer NH. Phytochemistry. 1985; 24:1747–1753.
19. Quijano L, Nuñez IS, Fronczek FR, Fischer NH. Phytochemistry. 1997; 45:769–775.
20. Smith CM, Kester KM, Fischer NH. Biochemical Systematics and Ecology. 1983; 11:377–380.
21. Klimash JW, Fischer NH. Phytochemistry. 1981; 20:840–842.
22. Lee K-H, Huang E-S, Piantadosi C, Pagano JS, Geissman TA. Cancer Res. 1971; 31:1649–1654. [PubMed: 4330633]
23. Ma G, Khan SI, Benavides G, Schuhly W, Fischer NH, Khan IA, Pasco DS. Cancer Chemother. Pharmacol. 2007; 60:35–43. [PubMed: 17149609]
24. Risinger AL, Li J, Bennett MJ, Rohena CC, Peng J, Schriemer DC, Mooberry SL. Cancer Res. 2013; 73:6780–6792. [PubMed: 24048820]

25. Tinley TL, Randall-Hlubek DA, Leal RM, Jackson EM, Cessac JW, Quada JC Jr, Hemscheidt TK, Mooberry SL. Cancer Res. 2003; 63:3211–3220. [PubMed: 12810650]

26. Steegmaier M, Hoffmann M, Baum A, Lénárt P, Petronczki M, Krššák M, Gürtler U, Garin-Chesa P, Lieb S, Quant J, Grauert M, Adolf GR, Kraut N, Peters J-M, Rettig WJ. Current Biology. 2007; 17:316–322. [PubMed: 17291758]

27. Boyd, MR.; Paull, KD.; Rubinstein, LR. Cytotoxic Anticancer Drugs: Models and Concepts for Drug Discovery and Development. Valeriote, FA.; Corbett, T.; Baker, L., editors. Amsterdam: Kluwer Academic Publishers; 1992. p. 11-34.

28. Skehan P, Storeng R, Scudiero D, Monks A, McMahon J, Vistica D, Warren JT, Bokesch H, Kenney S, Boyd MR. J. Natl. Cancer. Inst. 1990; 82:1107–1112. [PubMed: 2359136]

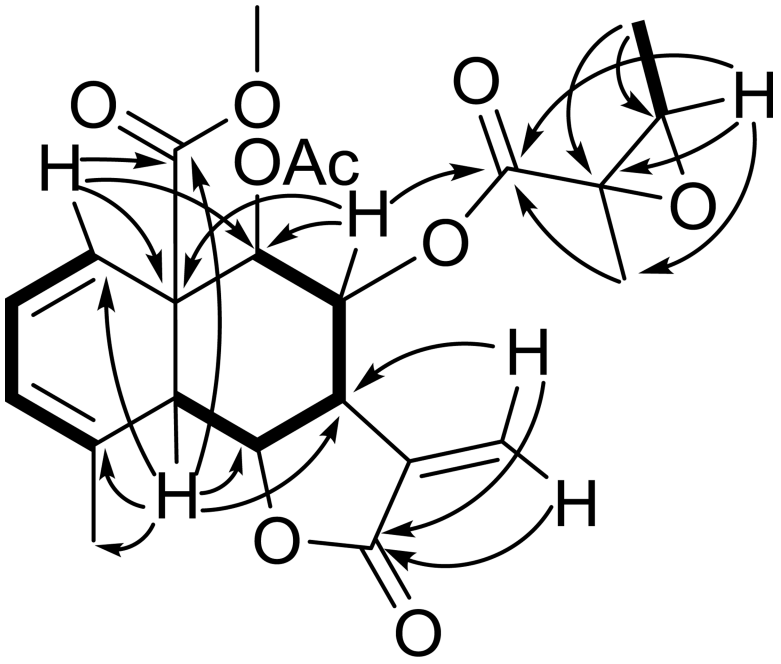

Figure 1.
Key HMBC (arrows) and COSY (bold) correlations of (**1**).

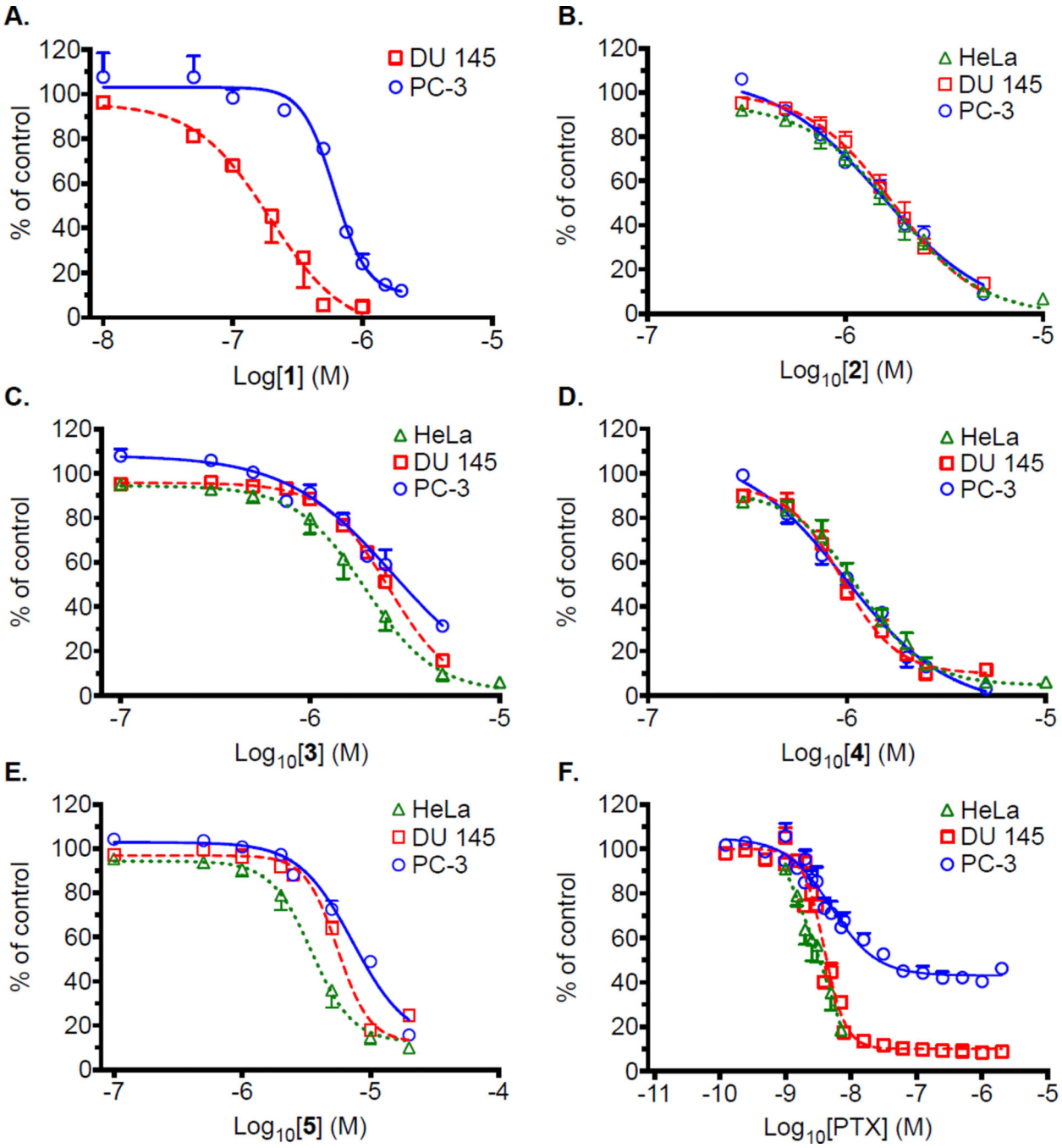

Figure 2.

Concentration-response curves for growth inhibition of PC-3, DU 145 and HeLa cells by compounds **1**–**5** or paclitaxel (PTX), measured with the SRB assay. Results represent n = 2–9 independent experiments, with each concentration tested in triplicate.

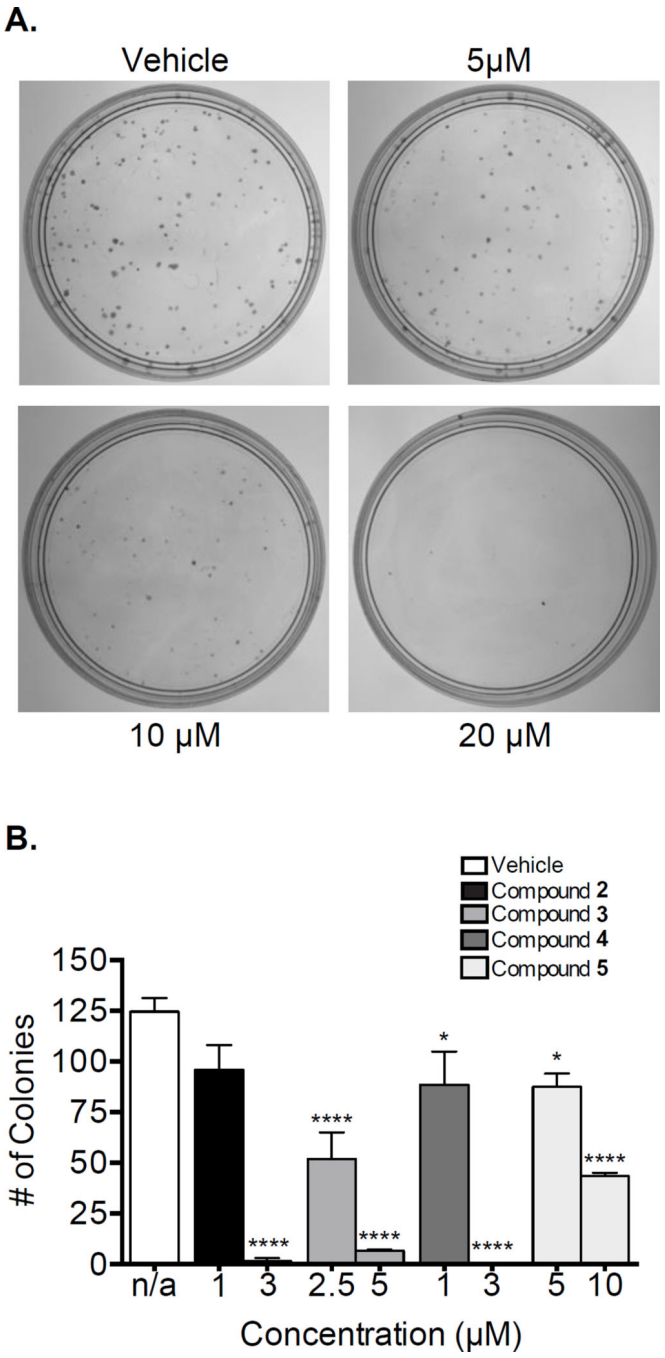

Figure 3.

Effects of a 4 h exposure to **2**–**5** on colony formation. DU 145 cells were treated with vehicle (DMSO) or a range of concentrations of **2**–**5** for 4 h before compound removal. Representative images of DU 145 colonies after 9 days of treatment with vehicle or **5** (A). Quantification of colony number after treatment with vehicle or **2**– **5** (B). *$p < 0.05$; ****$p < 0.0001$ compared to vehicle control; one-way ANOVA with Dunnett's post-hoc test. Results represent $n = 2$–9 independent experiments.

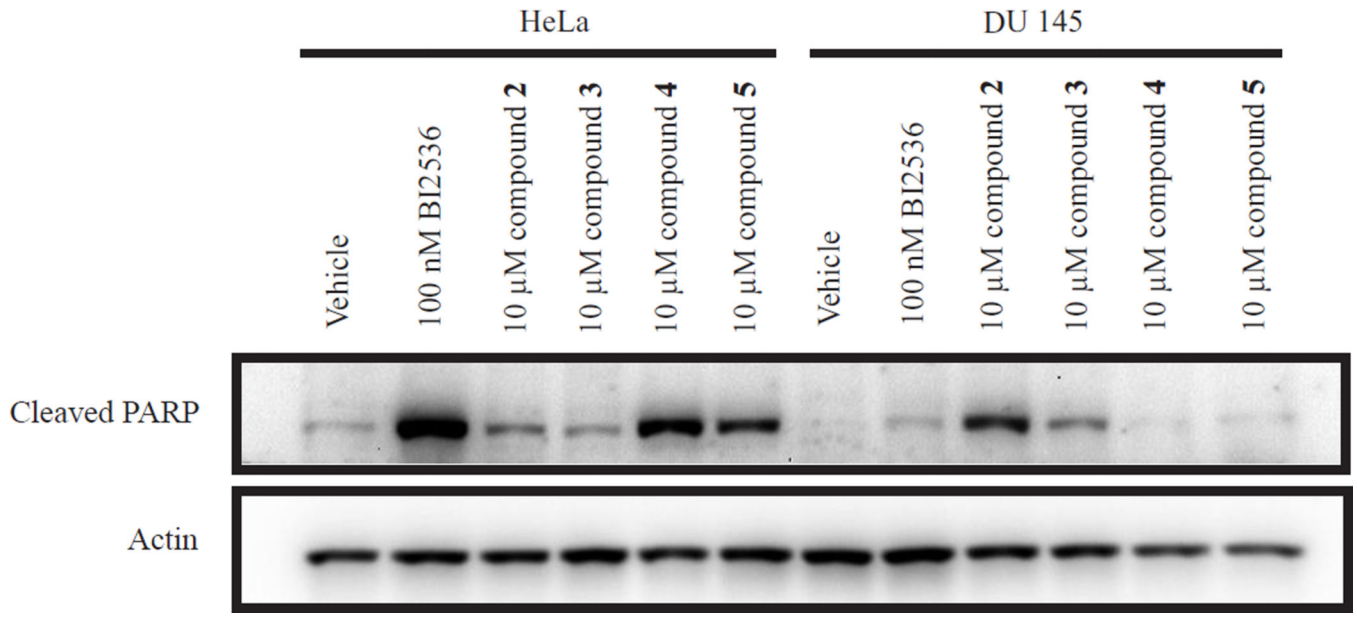

Figure 4.

Induction of PARP cleavage in HeLa and DU 145 cells by **2**–**5**. Cells were treated with the indicated concentrations of each compound for 24 h prior to lysis, SDS-PAGE and immunoblotting.

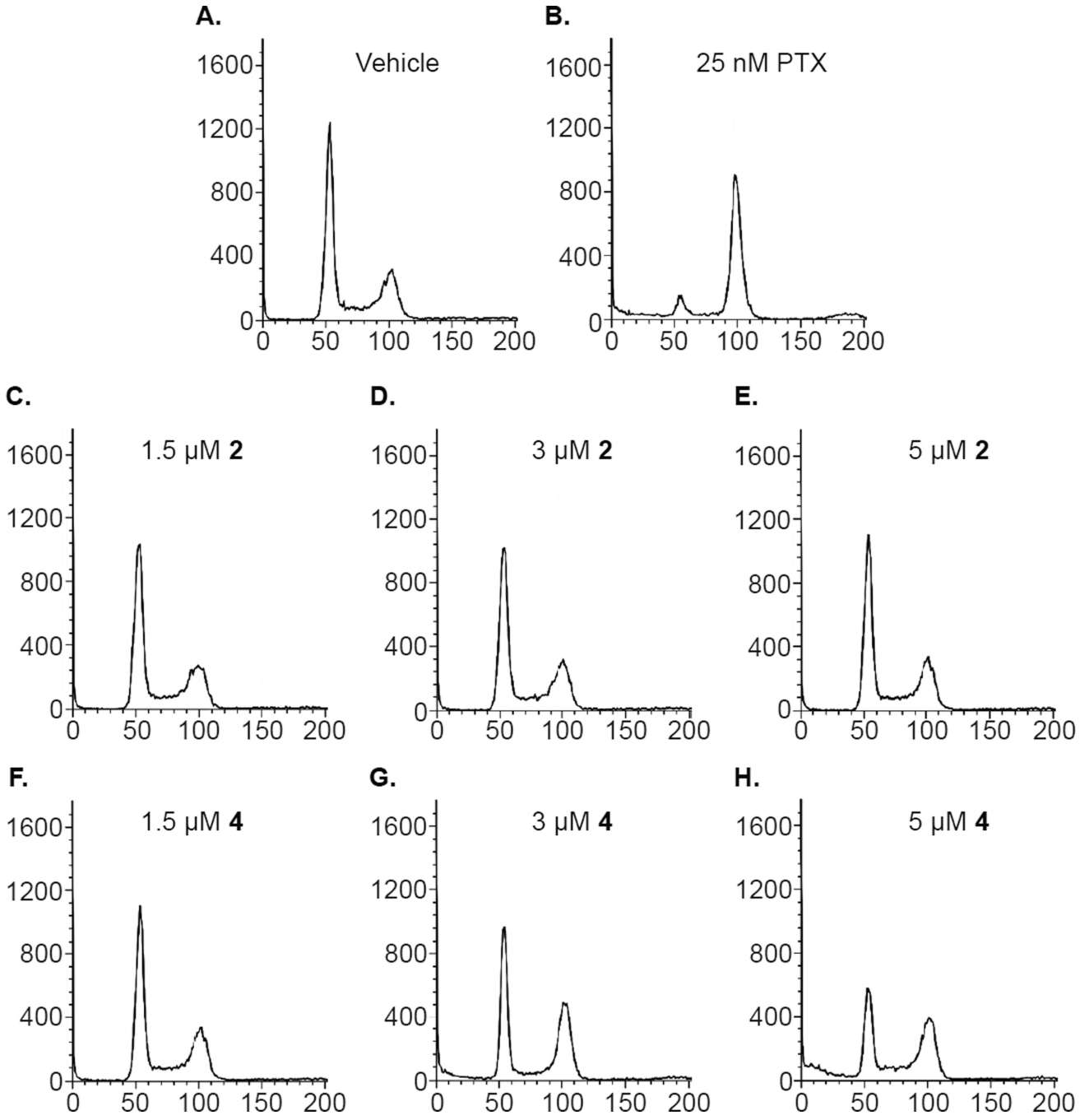

Figure 5.

Effects of **2** and **4** on cell cycle distribution of PC-3 cells after 18 h of treatment with vehicle, paclitaxel (PTX), **2** or **4**. Cells were treated as indicated for 18 h before staining with propidium iodide and analysis by flow cytometry.

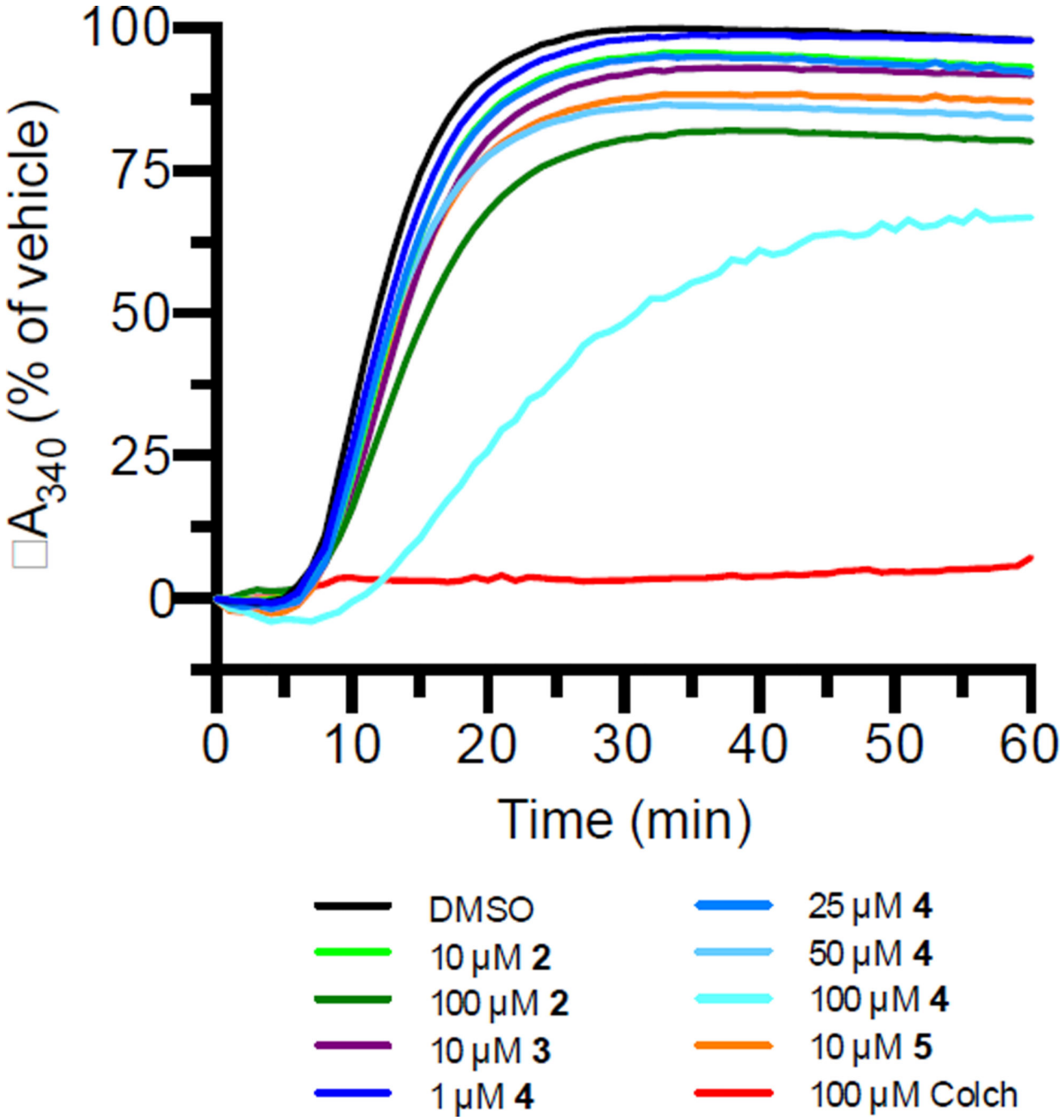

Figure 6.

Effects of **2**–**5** on purified tubulin polymerization in vitro. The polymerization of 2 mg/mL porcine tubulin was monitored turbidimetrically (A_{340}) in the presence of vehicle, **2**–**5** or colchicine for 60 min.

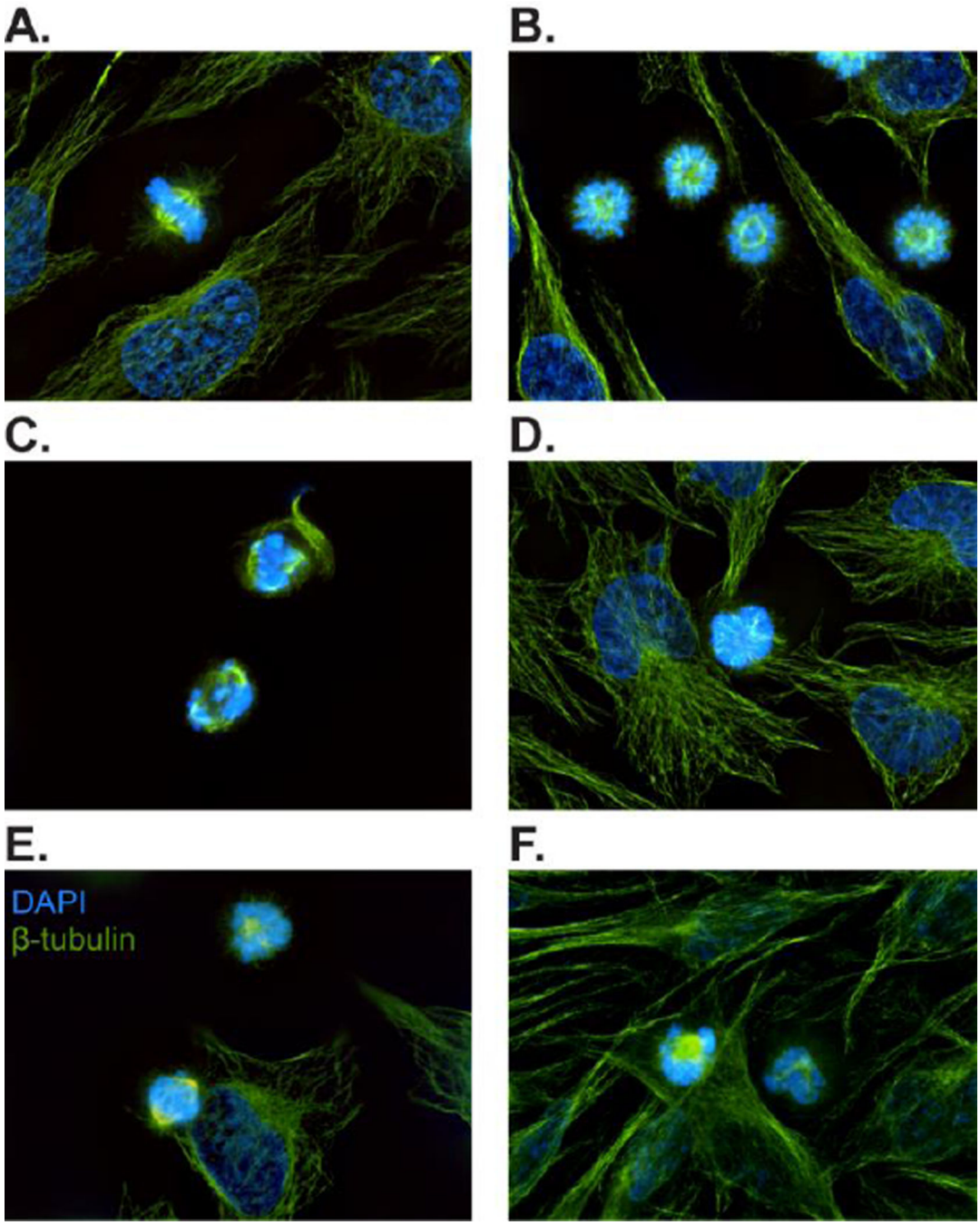

Figure 7.

Representative immunofluorescence images of HeLa cells after treatment with vehicle (A), 100 nM PLK-1 inhibitor BI2536 (B), 10 μM **2** (C), 7.5 μM **3** (D), 5 μM **4** (E) and 25 μM **5** (F). DNA was labelled with DAPI (blue) and microtubules were labeled with a monoclonal anti-β-tubulin antibody and FITC-conjugated anti-mouse IgG (green).

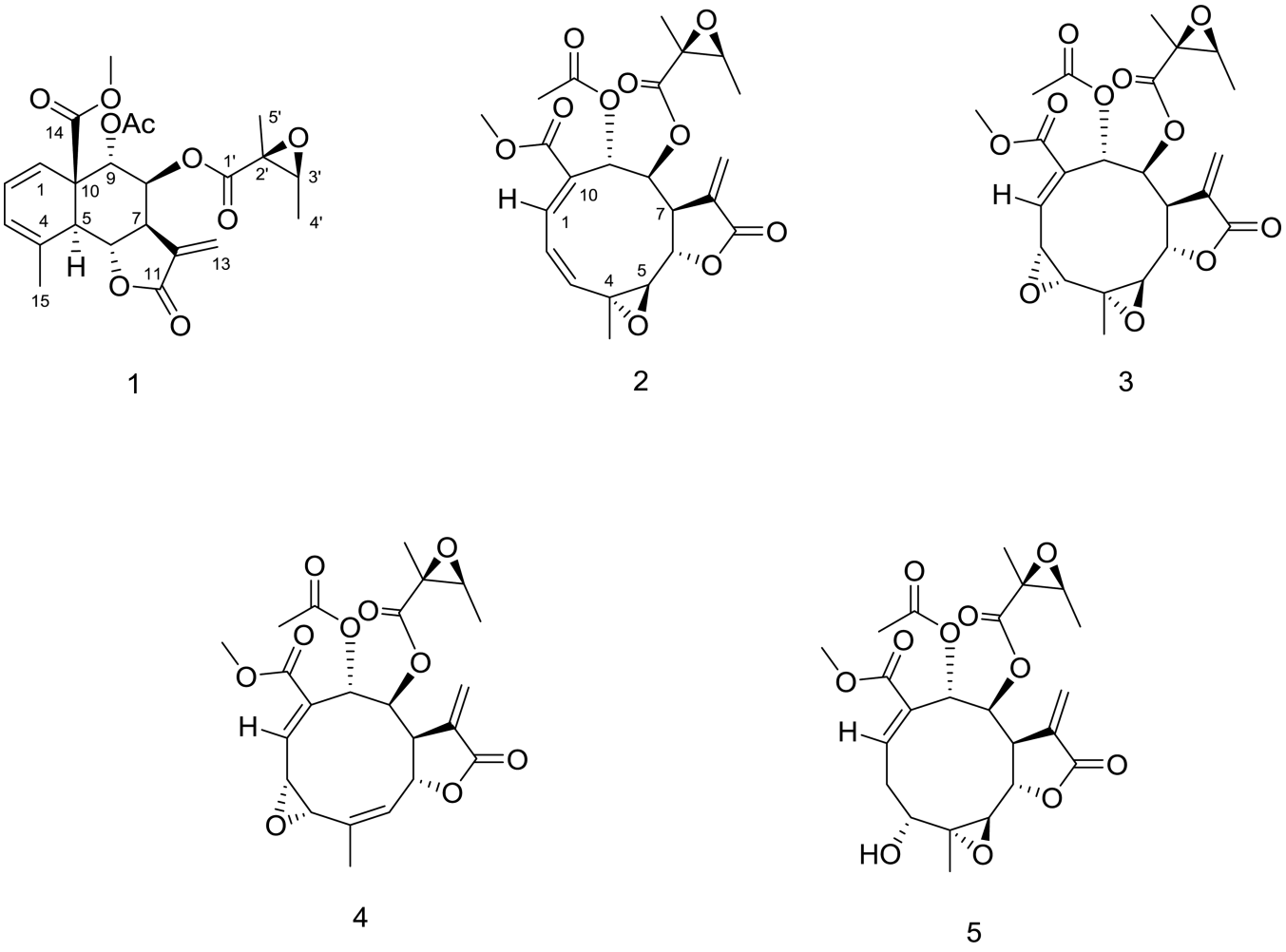

Figure 8.

Table 1

IC_{50} Values for Growth Inhibition of Cell Lines by Compounds 1–5 and Paclitaxel.

	IC_{50} ± SE (μM)			
compound	**PC-3**	**DU 145**	**HeLa**	**A-10**
meleucanthin (**1**)	0.67 ± 0.01	0.18 ± 0.04	N.D.	N.D
leucanthin-A (**2**)	1.7 ± 0.1	1.8 ± 0.2	1.7 ± 0.2	1.7 ± 0.4
leucanthin-B (**3**)	3.1 ± 0.3	2.6 ± 0.2	1.9 ± 0.3	1.1 ± 0.3
melampodin-A acetate (**4**)	1.1 ± 0.1	1.0 ± 0.1	1.1 ± 0.1	1.5 ± 0.5
3α-hydroxyenhydrin (**5**)	8.7 ± 0.6	5.9 ± 0.3	3.8 ± 0.6	3.0 ± 0.8
paclitaxel	0.04 ± 0.02	0.0040 ± 0.0004	0.0035 ± 0.0006	N.D

Table 2

IC_{50} Values for Growth Inhibition of Drug-Sensitive SK-OV-3 and Multidrug-Resistant SK-OV-3/MDR-1-M6/6 Cell Lines and the Associated Relative Resistances (Rr).

	IC_{50} ± SD (nM)		
compound	**SK-OV-3**	**SK-OV-3/MDR-1-M6/6**	**Rr[a]**
leucanthin-A (**2**)	570 ± 60	1400 ± 200	2.5
leucanthin-B (**3**)	820 ± 30	2000 ± 500	2.4
melampodin-A acetate (**4**)	390 ± 40	800 ± 100	2.1
3α-hydroxyenhydrin (**5**)	1700 ± 100	4400 ± 800	2.6
paclitaxel	6.2 ± 0.2	1010 ± 30	162.9

[a] Rr values calculated by dividing the IC_{50} in SK-OV-3/MDR-1-M6/6 cells by the IC_{50} in SK-OV-3 cells.